Published in : Semiconductor Science & Technology (2000), vol. 15, pp. 341-348.
Status : Postprint (Author's version)

Electrical conduction by interface states in semiconductor heterojunctions

M El Yacoubi, R Evrard, N D Nguyen and M Schmeits

Institute of Physics, B5 University of Liège, B4000 Sart Tilman/Liège 1, Belgium

Abstract

Electrical conduction in semiconductor heterojunctions containing defect states in the interface region is studied. As the classical drift-diffusion mechanism cannot in any case explain electrical conduction in semiconductor heterojunctions, tunnelling involving interface states is often considered as a possible conduction path. A theoretical treatment is made where defect states in the interface region with a continuous energy distribution are included. Electrical conduction through this defect band then allows the transit of electrons from the conduction band of one semiconductor to the valence band of the second component. The analysis is initiated by electrical measurements on n-CdS/p-CdTe heterojunctions obtained by chemical vapour deposition of CdS on (111) oriented CdTe single crystals, for which current-voltage and capacitance-frequency results are shown. The theoretical analysis is based on the numerical resolution of Poisson's equation and the continuity equations of electrons, holes and defect states, where a current component corresponding to the defect band conduction is explicitly included. Comparison with the experimental curves shows that this formalism yields an efficient tool to model the conduction process through the interface region. It also allows us to determine critical values of the physical parameters when a particular step in the conduction mechanism becomes dominant.

1. Introduction

The understanding of electrical conduction through semiconductor heterojunctions is of basic interest as many devices such as heterojunction bipolar transistors, heterojunction LEDs and lasers as well as photodetectors or solar cells contain such junctions between two different semiconductors . The efficiency of the conduction mechanism determines the performance of any device [1].

The electrical conduction in these systems cannot be in all cases interpreted by a classical drift-diffusion mechanism. Tunnelling through defect states in the interface region is often suggested as a possible conduction path. The object of the present paper is to propose a theoretical modelling of the conduction mechanism by including defects in the interface region with a continuous energy distribution. The charge carriers are then allowed to transit through this defect band from the conduction band of one component to the valence band of the other component.

The study is initiated by electrical measurements made on p-CdTe/n-CdS heterojunctions. Cadmium sulphide-cadmium telluride heterojunctions have received much attention as they are potential candidates for low-cost, highly efficient solar cells. The cells are generally made by successive deposition of thin films of CdS and CdTe. Despite their polycrystalline structure, high efficiencies, up to 15%, can be obtained [2]. These performances benefit from the optimum gap of 1.45 eV and the high absorption coefficient of CdTe. Cadmium sulphide with a bandgap of 2.42 eV is a useful window material for heterojunction solar cells.

The first part of the present paper is devoted to the experimental analysis of the electrical characteristics of p-CdTe/n-CdS heterojunctions obtained by chemical vapour deposition (CVD) of CdS onto single-crystal CdTe substrates. In such crystalline systems, effects such as recombination at grain boundaries are avoided. Nevertheless, the difference in crystalline parameters of about 10% is such that a high concentration of defects in the interface region is to be expected. In particular, dislocations extending over a thousand Ångstroms or more are possible. Atomic diffusion from one side of the heterointerface to the other is also possible.

Results of electrical characterization of CdTe/CdS heterojunctions have been reported in the literature [3-12]. In all cases, it does not seem possible to explain the observed characteristics by drift and diffusion as in p-n homojunctions. Tunnelling of electrons from the CdS conduction band to the CdTe valence band via interface

defect states has often been suggested to explain qualitatively the electrical conduction.

In the experimental part of this paper, we report results of measurements of dc current-voltage (*I-V*) characteristics, as well as of capacitance-frequency curves taken on samples of p-CdTe/n-CdS heterojunctions. These measurements were performed at different temperatures, from room temperature down to 200 K.

The interpretation of the results is made through a theoretical analysis based on the assumption of the existence in the interface region of defects with energy states in the common bandgap. If their concentration is large, these states may form a quasi-continuous energy distribution leading to a defect-state band. This is a way to represent an imperfect CdS overlayer grown on a CdTe substrate, with defect states present on both sides of the interface. In the model used for the calculations, the main contribution to the charge transport in the interface region under forward-bias conditions is due to electrons of the CdS conduction band which recombine on defect states in the CdS bandgap; from there they transit by conduction in the defect-state band to the CdTe side of the heterointerface where they recombine with holes from the p-CdTe valence band.

As will be shown, this numerical treatment constitutes an efficient way to simulate the various recombination, tunnelling and hopping mechanisms, which are most probably present. Due to the complexity of the mechanisms occurring at a real heterojunction a complete description including all intermediate steps of the current transport is not possible. Within the numerical modelling it is also possible to simulate various configurations corresponding to different parameter sets and to determine critical values of the parameters which determine basic macroscopic quantities such as those resulting from the electrical measurements.

The comparison between experimental and theoretical dc and ac characteristics shows that the model proposed in this paper can be useful for the study of electrical conduction in heterojunction systems.

2. Experimental results

Without discussing all the experimental details on the preparation conditions, let us just say that the CdS layers, about 0.2 μm thick, were grown by a simple chemical-vapour deposition technique on single crystals of p-type As-doped CdTe; the substrates are oriented parallel to (111) planes. To improve the n character of the CdS layers, vapour of $CdCl_2$ was introduced into the reactor during growth. Finally, we deposited In contacts onto the CdS surface of the samples by thermal evaporation in a vacuum of 2×10^{-6} Torr. We prepared ohmic contacts on the CdTe substrates by first treating the samples for 10 minutes in a solution of lithium nitrate in water, with a concentration of 10^{-4} mol m^{-1}. Then we used electroless deposition of gold to obtain contacts of relatively low resistance. These contacts have a surface of about 1 mm^2. Measurements between two such contacts on the same substrate show that they are ohmic with a resistance of 100 Ω at most.

Acceptor concentrations in CdTe substrates, as determined by Hall measurements, are about 4×10^{16} cm^{-3}. The donor concentration in the CdS layers, determined from *C-V* measurements, is about 2×10^{16} cm^{-3}.

We first measured the dc current-voltage characteristics of these samples between room temperature and 210 K. The current was limited to 0.1 mA to avoid sample breakdown.

Figure 1. *Experimental current-voltage curves for a typical sample at five different temperatures.*

Published in : Semiconductor Science & Technology (2000), vol. 15, pp. 341-348.
Status : Postprint (Author's version)

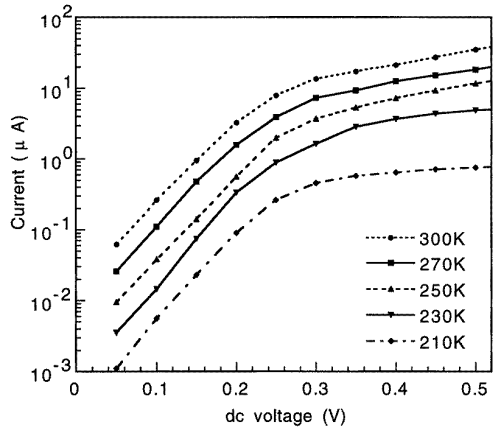

In figure 1 we show these current-voltage characteristics at five temperatures ranging from 210 to 300 K, for one sample. The other samples show the same characteristic behaviour. The convention of sign is such that positive voltages correspond to forward biased heterojunctions. Figure 4, which will be discussed later on, shows the band structure constructed in the framework of the usual model based on the difference of electron affinities and on the hypothesis of a neutral CdTe/CdS interface. Due to the relatively high energy barrier between the CdTe and CdS conduction bands, and the even higher barrier between the valence bands, the injection of minority carriers predicted within this model should remain negligible at weak bias. This is in contradiction with our observations. In the case of the sample discussed here for instance, we measure at room temperature a current of about 0.3 μA for a bias as weak as 0.1 V. This shows that the current transport through the heterojunction is certainly not due to thermal injection of minority carriers. This is confirmed by the examination of the behaviour of the *I-V* characteristics in terms of temperature. As shown in figure 1, the slope of the characteristic curves is almost temperature independent up to 0.3 V of applied voltage, in the linear region. This leads us to suggest, for this region, an *I-V* relation of the form

$$I = I_0 \exp(BV). \qquad (1)$$

We obtain that B is about 21 V^{-1} and almost completely independent of temperature. Therefore, the temperature dependence is mainly contained in the pre-exponential factor I_0.

All this suggests that conduction mechanisms other than thermal injection of minority carriers must exist. Moreover, the reverse voltage characteristics show no saturation, indicating also that defect-assisted generation or tunnelling mechanisms occur. Above 0.3 V of applied voltage, the *I-V* curves deviate from the characteristic exponential behaviour, which is indicative of a series resistance effect.

In figure 2, we show for values of V equal to 0.1, 0.2 and 0.3 V, the current as a function of the inverse thermal voltage q/kT. The results indicate that the conduction process is thermally activated with an activation energy which has only a weak dependence on the applied voltage. For the three values of V considered here, we find activation energies ε_a of respectively 0.32, 0.29 and 0.25 eV. This proves that changing the forward bias does not appreciably modify the band bending either in CdTe or in CdS. Therefore, the change in voltage due to an external source is almost entirely applied to a relatively thin interface layer.

We also have determined the ac-current characteristics for various values of temperature and applied steady-state voltage. As a typical result, we show in figure 3 for $T = 300$ K and $V = 0$ V the capacitance-frequency (C-f) curve of the CdTe-CdS junction. The C-f curve shows a decrease of the capacitance from 650 pF to 250 pF in the 10^2-10^4 Hz range and from 250 to 150 pF in the 10^4 to 10^6 Hz frequency range. A first analysis suggests the presence of a continuous distribution of defect states, with a resulting continuous distribution of cutoff frequencies, leading to a progressive decrease of the response of the defect states to the applied ac voltage.

Figure 2. *Experimental current-inverse thermal voltage curve for same sample as in figure 1, for values of the applied voltage equal to 0.1, 0.2 and 0.3 V.*

Published in : Semiconductor Science & Technology (2000), vol. 15, pp. 341-348.
Status : Postprint (Author's version)

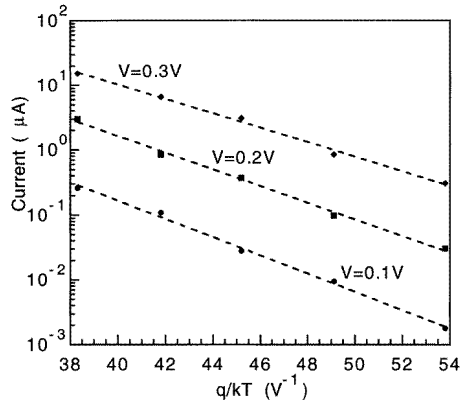

Figure 3. *Experimental capacitance—frequency curve for zero bias and T = 300 K.*

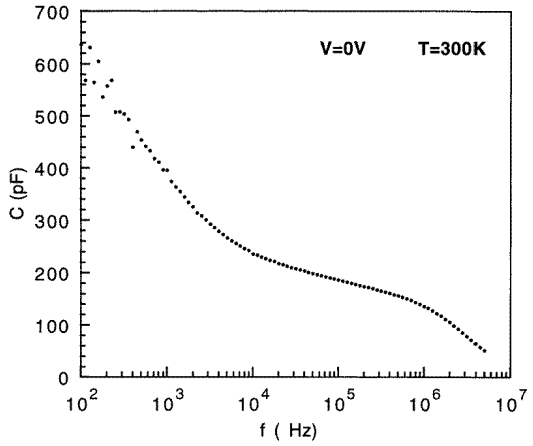

3. Theoretical analysis

The theoretical study is based on the numerical resolution of Poisson's equation and the continuity equations for electrons, holes and occupied defect levels [13, 14]. The experimental results lead us to propose the following model to explain the charge transport through the junction. Defect states located in the interface region form a continuous distribution of energy levels, with a density of states per unit energy $D_t(x, E_t)$. The defect states are supposed to interact strongly, so that their occupation can be described by a Fermi function $f_t(x, E_t)$ with a quasi-Fermi energy F_t for non-equilibrium situations. The detailed formal developments can be found in [13] and [14]. The occupation function for defect states at a given energy E_t is given by

$$f_t = \frac{1}{1 + g \exp[(E_t - F_t)/kT]} \qquad (2)$$

where g is the degeneracy factor. The local concentration of occupied states at a position x is given by

$$n_t(x) = \int_{E_v}^{E_c} f_t(E_t) D_t(E_t)\, \mathrm{d}E_t \qquad (3)$$

where E_v and E_c are the valence and conduction band edges. Integration over the bandgap of $D_t(x)$ yields the local total concentration of defect states $N_t(x)$.

We assume the existence of a physical mechanism allowing for a rapid spatial exchange of electrons between

neighbouring defect sites. In our model this is accounted for by introducing a current in the defect band. We assume that the current in the defect band is given by the expression

$$\vec{J}_t = n_t \mu_t \vec{\nabla} F_t \qquad (4)$$

where μ_t is the mobility of the electrons in the defect band. This expression leads to a current proportional to the gradient of the quasi-Fermi level F_t and is of course zero at thermal equilibrium. The form is similar to that used for the electron and hole currents in non-degenerate semiconductors [15].

Due to the conduction in this defect-state region, the electrons come to the interface where they recombine with holes from the CdTe valence band. The detailed mechanism of the electrical conduction by these defect states is not known at the atomic scale. It may be hopping motion or tunnelling between adjacent defects. What is important for our purpose is that equation (4) yields a tractable expression allowing us to simulate the effect of the conduction by the defect states in the numerical computation.

The electron mobility in the defect band μ_t is of course a parameter difficult to estimate, as it is not a directly measurable quantity. It will be shown that the results of the calculations are not very sensitive to the value chosen for μ_t, provided that it is not too small. One reason is that the conduction paths in the defect band are restricted to the near interface region, and thus are quite short. Another reason is that the capture and emission of charge carriers by the traps are the dominant mechanisms limiting the current in the junction.

The theoretical analysis of the junction is based on the numerical resolution of a set of four equations coupling the electrical potential ψ, the electron and hole concentrations n and p and the concentration of occupied states n_t. These are Poisson's equation and the continuity equations for electrons, holes and occupied defect states.

This latter equation is given by

$$\frac{\partial n_t}{\partial t} = R_{nt} - R_{pt} + \frac{1}{q}\vec{\nabla} \cdot \vec{J}_t \qquad (5)$$

where R_{nt} is the transition rate for exchange of electrons with the conduction band and R_{pt} that for exchange of holes with the valence band. We assume that these exchanges can be described by the usual expressions resulting from capture and emission according to the Shockley-Read-Hall recombination scheme [14]. Then R_{nt} is the transition rate resulting from the difference between the integrated electron capture rate and the integrated electron emission rate

$$R_{nt}(x) = \int_{E_v}^{E_c} r_{nt}(E_t, x)\, \mathrm{d}E_t \qquad (6)$$

$$\text{with} \quad r_{nt}(E_t) = c_n n(1 - f_t)D_t - e_n f_t D_t. \qquad (7)$$

Similarly, the defect to valence band transition rate $R_{pt}(x)$ can be written with $r_{pt}(E_t)$ given by

$$r_{pt}(E_t) = c_p p f_t D_t - e_p(1 - f_t)D_t. \qquad (8)$$

In the above relations c_n and c_p are the electron and hole capture coefficients, related to the electron and hole capture cross sections by $c_n = \upsilon_{th}{}^n \sigma_n$ and $c_p = \upsilon_{th}{}^p \sigma_p$, where υ_{th} are the respective thermal velocities. The relations between c_n, c_p and the electron and hole thermal emission rates e_n and e_p are given by the following equations, expressing microreversibility between individual states at thermal equilibrium.

$$e_n = g c_n N_c \exp[(E_t - E_c)/kT] \qquad (9)$$

$$e_p = \frac{c_p}{g} N_v \exp[(E_v - E_t)/kT]. \qquad (10)$$

In the numerical study of the p-CdTe/n-CdS heterojunctions we have taken the dopant concentrations

respectively equal to $N_A = 4 \times 10^{16}$ cm^{-3} and $N_D = 2 \times 10^{16}$ cm^{-3}, in accordance with the experimental values. As the system has a planar symmetry, we use a one-dimensional analysis, where the distances from the interface are measured by a variable x, with $x = 0$ at the position of the heterointerface. The x-axis is oriented in the direction of the CdS epitaxial film.

The first results we show are obtained with the following choice of parameters. We take the conduction band discontinuity ΔE_C equal to 0.22 eV, the value estimated from the difference in electron affinities of CdTe and CdS [11]. All other parameters describing bulk properties correspond to common values of CdTe and CdS [15]. The defect band mobility is taken equal to 10^{-3} times the electron mobility in CdTe. For the electron and hole capture cross sections, we use energy-independent values $\sigma_n = \sigma_p = 5 \times 10^{-15}$ cm^2. The defect states are supposed to be acceptor-like, in the sense that they are neutral when empty and negatively charged when occupied.

For the defect distribution function D_t, we choose a constant value in a band of width $\Delta E_t = 0.7$ eV located 0.21 eV below the CdS conduction band edge, 0.54 eV below the CdTe conduction band edge. The x-dependence of the density of states is such that $N_t(x)$ is constant and equal to 1×10^{17} cm^{-3} for values of x between -0.01 μm and +0.1 μm. Beyond this last value, N_t decreases linearly to zero between +0.1 and +0.2 μm. This simulates a defect band existing on both sides of the interface, with a larger extent in the CdS layer, as can be expected in the case of films grown on substrates with a large lattice mismatch.

Figure 4. *Energy band diagram for CdTe-p/CdS-n heterojunction at V = 0.2 V applied voltage. The interface defect band extends from x = -0.01 to 0.2 μm. The total defect concentration is $N_t = 10^{17}$ cm^{-3} for x = -0.01 μm to 0.1 μm, and goes linearly to zero from x = 0.1 to 0.2 μm. $N_t = 0$ outside that region. The defect density of states $D_t(x, E_t)$ is constant as a function of E_t, over a width $\Delta E_t = 0.7$ eV.*

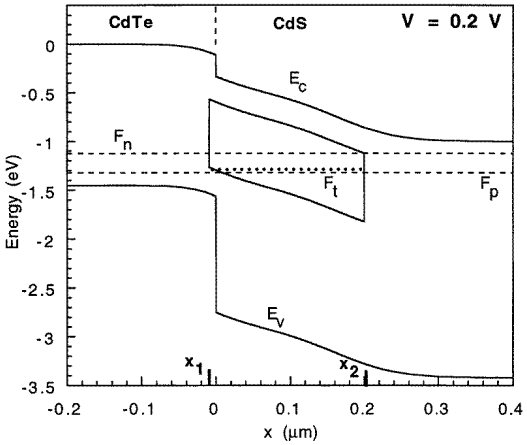

Figure 4 gives the result of our calculations for the energy-band diagram in the interface region, and a steady-state applied voltage of $V = 0.2$ V. In the range of values of x represented in the figure, i.e. from -0.2 to 0.4 μm, the electron and hole quasi-Fermi levels F_n and F_p are nearly constant and separated by 0.2 eV. They join for x-values outside the figure as usual. The defect quasi-Fermi level F_t is nearly flat in the whole defect region, with a position intermediate between F_n and F_p, indicating that, for the chosen set of parameters, the defect states are in equilibrium with neither of the two bands.

In figure 5 we show, for the same value of the applied voltage, the recombination rates R_{nt} and R_{pt} as functions of the position x, alongside with the different current densities J_n, J_p and J_t. These figures clearly reveal the conduction mechanism of the junction. When the electrons injected from the n-CdS side reach the defect region, they are captured by the defect traps. These capture transitions take place for x between 0.15 μm and 0.20 μm, i.e. in the region where the concentration of traps has not yet reached its maximum value. As figure 5(a) shows, the capture rate of electrons by defects R_{nt} is maximum near the boundary of the region with defect states in the CdS layer and decreases rapidly when going towards the interface with CdTe. After capture, the electrons are swept through the defect band up to the heterointerface at $x = 0$, where they recombine with the holes on the p-CdTe side of the junction. As figure 5(b) shows, below 0.15 μm the current is almost entirely due to the transport

of electrons via trap states. Indeed the total current density J is such that $J = J_t$ for this CdS region close to the interface. In the small layer of 0.01 μm where the defect layer is allowed to extend on the CdTe side in our model, the current transforms from a defect dominated contribution J_t to a hole current J_p, due to the strong hole transition rate R_{pt} which appears in figure 5(a). Beyond this x value, the current is transported by holes exclusively.

This conduction mechanism is of course much more efficient than a thermally activated emission over the energy barrier. Indeed, for an electron, the energy barrier is of the order of the built-in potential plus AE_c, the conduction band discontinuity, i.e. about 1 eV. The barrier is even higher for the holes. In contrast, within our model, the part of the process that is thermally activated is the transport of electrons and holes from their respective ohmic contact to the recombination region, which is close to the limits of the defect region. This requires little thermal activation, typically a few hundreds of meV, as will appear from the analysis of the current-voltage values for different temperatures.

Figure 5. *(a) Conduction band to defect state transition rate R_{nt} and defect state to valence band transition rate R_{pt}, as a function of x, for forward biased junction, with V = 0.2 V. (b) Current densities for electrons J_n, holes J_p and defect band J_t, and total current density J for applied voltage V = 0.2 V.*

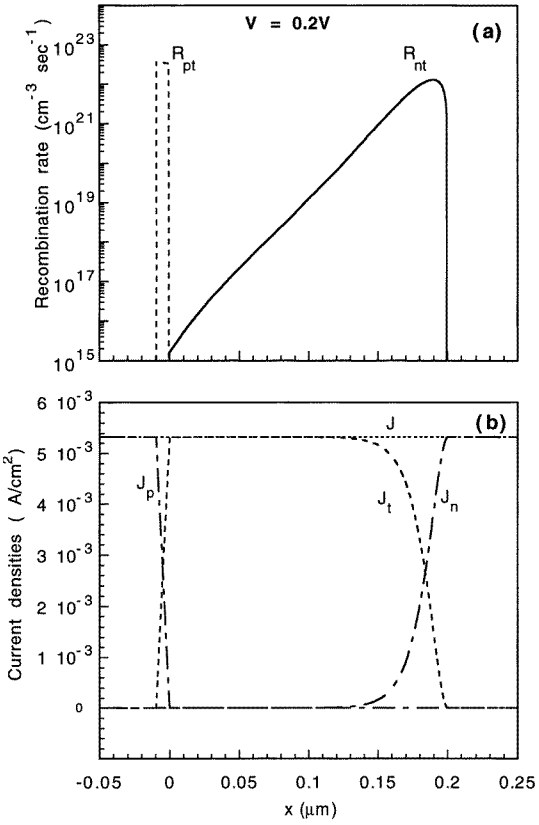

Figure 6. *Theoretical current density J as function of inverse thermal voltage q/kT for the system described in figure 4, for three values of applied voltage.*

Published in : Semiconductor Science & Technology (2000), vol. 15, pp. 341-348.
Status : Postprint (Author's version)

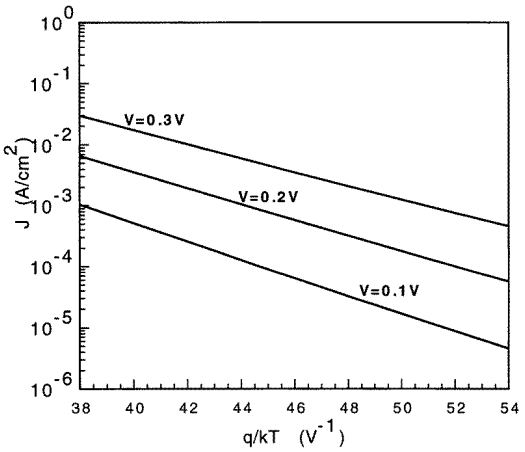

Figure 6 shows the logarithm of the calculated total current densities J as functions of the inverse thermal voltage q/kT, for three values of the applied voltage V = 0.1, 0.2 and 0.3 V. Notice that, for this temperature range, log J is a linear function of q/kT. The activation energies which can be deduced from the slope of the functions are respectively 0.34 eV for V = 0.1 V, 0.30 eV for V = 0.2 V and 0.26 eV for V = 0.3 V. As can be inferred from figure 4, these activation energies correspond to mean values of the barrier felt by the electrons on the n-CdS side of the junction. The thermal activation of electrons is the transport-limiting mechanism as the valence band edge on the CdTe side is nearly flat.

Comparing with the experimental results shown in figure 2, one retrieves the linear slope of the log I-q/kT curves, with similar values of the activation energies. Even the absolute values of the currents are comparable. Indeed the junctions studied experimentally have sections of about 1 mm^2, leading to current densities of the same order of magnitude as those of figure 6.

Figure 7. *Current density at T = 300 K, V = 0.2 V applied dc voltage for defect concentration N, as described in figure 4, for different values of the parameter sets* $\varepsilon_{\mu t} = \mu_t/\mu_{t0}$, *with* $\mu_{t0} = \mu_n(CdTe) \times 10^{-3}$, $\varepsilon_n = \sigma_n(CdS)/\sigma_{n0}$, $\sigma_{n0} = 1 \times 10^{-15}$ cm^2 *and* $\varepsilon_p = \sigma_h(CdTe)/\sigma_{p0}$, *with* $\sigma_{p0} = 10^{-15}$ cm^2. *When one parameter is modified, the two others are kept equal to their standard values.*

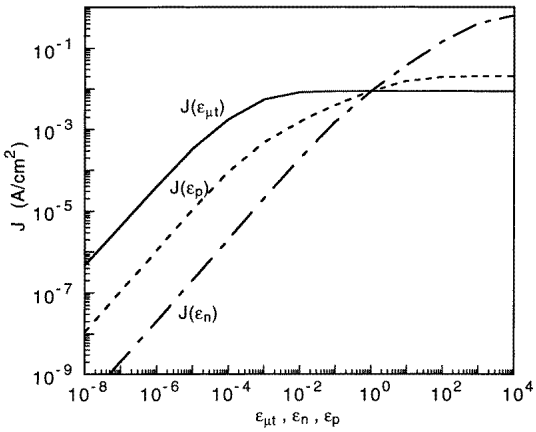

The conduction process depends on a series of parameters which describe the different steps and which are difficult to estimate from basic principles or to obtain from direct experimental measurements. Therefore we show the effect of some of these parameters on basic dc characteristics. In figure 7, we show the resulting current at 300 K and 0.2 V of applied voltage as a function of the defect band mobility μ_t, the electron capture cross

section σ_n of CdS and the hole capture cross section of CdTe σ_p. The abscissa are normalized values $\varepsilon_{\mu t}$, ε_n and ε_p of the three parameters with the set of parameters of figure 4 taken as reference values. Modifying one of the three values $\varepsilon_{\mu t}$, ε_n or ε_p, keeping all others fixed, yields the three curves $J(\varepsilon)$. They show that the modification of the defect band mobility μ_t only leads to a sizeable effect when μ_t is reduced by at least a factor 10^{-4}. Decreasing the electron and hole capture cross sections σ_n and σ_p relative to the reference value produces important modifications of the resulting current, as expected. Increasing σ_p with respect to the reference value modifies only slightly the current value, whereas increasing the electron capture cross section σ_n of CdS produces a further increase of the current. This illustrates that within this parameter region, the filling of the defect states is effectively the current-controlling part of the conduction mechanism.

Other important parameters describing the defect states are those related to the defect distribution function D_t, with its energy dependence and its spatial extension. The effect of the extension x_2 of the defect region on the CdS side is illustrated in figure 8, where three different values of the defect density of states width ΔE_t are considered. The integrated value $N_t(x)$ and all other parameters are kept equal to those of the reference system. For $V = 0.2$ V of applied voltage and $\Delta E_t = 0.5$, 0.7 and 0.7 eV, we have determined the thermal activation energy resulting from the computed values of the current as a function of $1/T$, modifying the value of x_2 between 0.1 μm and 0.3 im. The curves show that in all cases, the activation energies decreases when x_2 increases, which is a result of the modification of the shape of the conduction band edge on the CdS side of the junction. The value of 0.3 eV suggested by the experiment, is best reproduced with $x_2 = 0.2$ μm and a defect band width of $\Delta E_t = 0.7$ eV. Considering other values of the applied voltage yields similar agreement for the corresponding activation energies. These results justify the choice of parameters we have used for figure 4 and the resulting curves. Due to the large number of parameters, several combinations of parameters could yield valuable comparison with experiment. As shown by figure 8, taking $\Delta E_t = 0.9$ eV instead of 0.7 eV could be another plausible solution.

In order to determine the capacitance-frequency curves, we have performed a small-signal ac analysis which consists in solving the same set of basic equations in response to an applied voltage consisting of a steady-state component V_0 plus a harmonic component of amplitude ϋ and frequency $\omega = 2\pi f$. Within the small-signal approximation, all quantities can be written as the sum of a steady-state dc component and a sinusoidal ac component [14]. The electron concentration for example can be written

$$n(x,t) = n^0(x) + \tilde{n}(x)\,\mathrm{e}^{\mathrm{i}\omega t}. \qquad (11)$$

Figure 8. *Activation energy ε_a at $V = 0.2$ V applied dc voltage, $T = 300$ K as a function of x^2, the width of the defect region on the CdS side of the junction. The three curves correspond to the same value of the integrated defect density N_t, but with different width of the defect density of states function ΔE_t. The experimental activation energy is $\varepsilon_a = 0.29$ eV.*

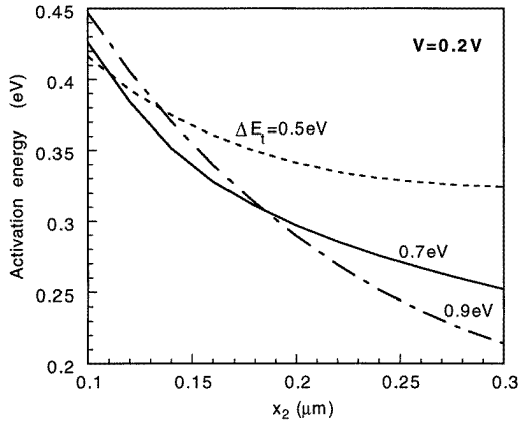

Figure 9. *(a) Electron, hole and occupied defect state densities at steady state for $V = 0$ V (dotted curves) and real part of small signal amplitude of low-frequency ac component of the same quantities, as a function of position x. (b) Real and imaginary part of electron, hole, displacement and defect current densities as a function*

of position x.

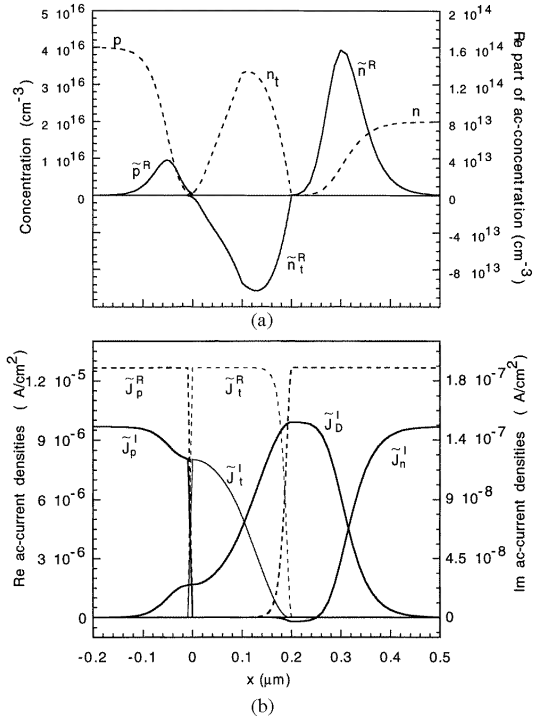

In figure 9(a) we show for $V = 0$, as a function of position x, the steady-state concentrations of electrons, holes and occupied defect levels n_t, together with the real part of the low-frequency response of the same quantities. At this frequency, the imaginary part is orders of magnitude weaker. The figure shows that the modification of the electron and hole concentration at the depletion layer edges occurs while the defect concentration is modified, but with opposite sign. The *x*-integration of the real part of the ac-value of $n(x)$ - $nt(x)$ - $p(x)$ yields zero, thus ensuring charge conservation and electrical neutrality.

Figure 9(b) shows the real and imaginary parts of the different current components, namely the electron and hole currents J_n and J_p, the defect band current J_t, as well as the displacement current J_D. This latter makes that the total current is constant as a function of *x*. The real parts correspond to the resistive part of the current and have the same slope as the dc components already shown in figure 5. The imaginary parts correspond to the capacitive part of the current and illustrate well the respective filling and emptying of the conduction band, valence band and defect states as appears in figure 9(a). This already indicates that the capacitance, which is determined by the modification of the space charge with applied voltage will depend on the way the charge on the defect states is modified. Usually this occurs by only local exchange of electrons with the conduction band or of holes with the valence band, but here displacement of mobile electrons inside the defect band contributes too.

This is further illustrated in figure 10, where we show the calculated $C(f)$ curves for different values of the defect-band mobility μ_t. It is seen that when μ_t is set equal to zero, the $C(f)$ curve shows a continuous decrease up to 10^5 Hz. Increasing the mobility μ_t produces an increasing value of the low-frequency capacitance and a steplike shape with a cutoff frequency moving towards higher frequencies when μ_t increases. In figure 11 we show in a way similar to figure 7, the cutoff frequencies as a function of the relative values of the defect band mobility $\varepsilon_{\mu t}$, the CdS electron capture cross section σ_n and the CdTe hole capture cross section σ_p. The cutoff frequency is defined as the frequency for which the capacitance takes the mean value between the low-frequency capacitance and the high-frequency capacitance. In the case of discrete bulk defects, it corresponds to the frequency above which the defect states no longer respond to the applied voltage. The figure shows that below the reference set of parameters, it is the hole capture cross section σ_p in CdTe which allows us to modify the cutoff frequency. Above the reference value, both electron and hole capture cross sections allow us to increase the cutoff frequency. The defect band mobility must be modified by at least a factor of 10^3 to produce a reduction of the response of the hole defect state system.

Comparison with the experimental $C(f)$ curve requires great care. It is effectively difficult to reproduce experimentally the steplike shape with a constant value of the $C(f)$ function beyond the cutoff frequency [16]. In our case, the fact that the experimental curve of figure 3 is not reproduced by one of the shown theoretical curves

seems to indicate that the real system is even more complicated than we assumed. Beside the states that we have included to explain the dc-current behaviour, there must exist another distribution of defect states whose population is modified when an ac voltage is applied to the system. They should yield a contribution to the capacitance, without participating in the dc conduction mechanism. This could for example be described by a mechanism where one of the three steps occurring in our model of the current transport is forbidden. The C(*f*) curve a in figure 10 shows such a behaviour.

Figure 10. *Theoretical capacitance-frequency curves for V = 0, T = 300 K for CdTe-p/CdS-n heterojunction as described in figure 4 (curve a), values of the relative defect mobility $\varepsilon_{\mu t} = 0$ (curve a), 10^{-6} (b), 10^{-4} (c), 3×10^{-4} (d), 10^{-3} (e) and 1 (f).*

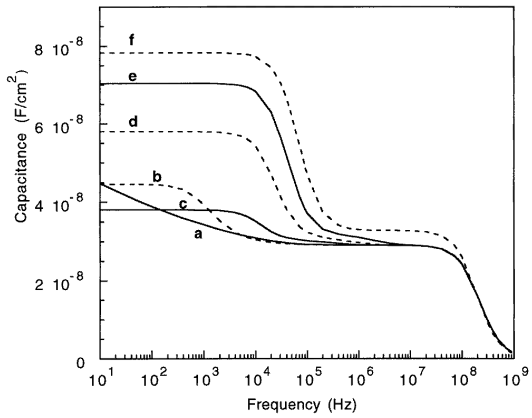

Figure 11*. Theoretically determined cutoff-frequency ω_c for different values of the relative value of the parameters $\varepsilon_{\mu t}$, ε_n, ε_p as defined in figure 7.*

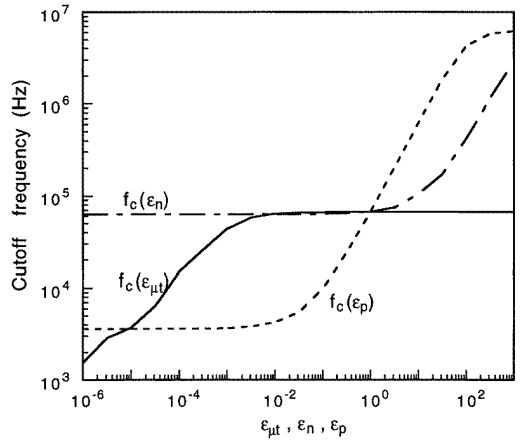

4. Conclusion

We have presented a way of modelling electrical conduction mediated by interface states in a semiconductor heterojunction. The analysis starts from an experimental study of electrical characteristics of CdTe/CdS heterojunctions. The interpretation was made by a numerical analysis based on a model including conduction through a band of defect states in the interface region. In a forward biased junction, the electrons are injected from the CdS-n side of the junction into the defect band, which performs the current transport towards the CdTe-p valence band.

This model correctly explains conduction in the dc regime, at least for the low-voltage linear region. The analysis of our model shows that the electrons are captured by the defect states relatively far from the interface with CdTe. This explains the small value of the activation energy in the mechanism of charge transport, as well

as the fact that the slopes of the curves giving log *I* against *V* are almost independent of temperature.

The experimentally obtained *C-f* behaviour suggests the presence of a distribution of defect states with varying energy position inside the gap. The theoretical study allows us to analyse a defect dependent behaviour of the ac response of the junction. It suggests that the model should be refined by adding a second group of interface states which would interact with the bands without participating in the defect band conduction.

The results show that the inclusion of a current in the defect state band represents an efficient tool in the study of the electrical characteristics of semiconductor heterojunctions, where a full treatment taking into account the presence of interface states is otherwise nearly impossible, if one wants to describe a real system.

Acknowledgment

Financial support of the Belgian Fonds National de la Recherche Scientifique (contract 9.4565.96F) is gratefully acknowledged.

References

[1] Morgan V and Williams R H (eds) 1991 *Physics and Technology of Heterojunction Devices (IEE Materials and Devices Series 8)* (London: Peregrinus)

[2] Partain L D1995 *Solar Cells and their Applications* (New York: Wiley)

[3] Ou S S, Stafsudd O M and Basol B M 1984 *Solid State Electron.* 27 21

[4] Anthony T C, Fahrenbuch A L, Peters M G and Bube R H 1985 *J. Appl. Phys.* 57 400

[5] Chu T L, Chu S S and Ang S T 1988 *J. Appl. Phys.* 64 1233

[6] Ercelebi C, Brinkman A W, Furlong T S and Woods J 1990 *J. Cryst. Growth* 101 162

[7] Ringel S A, Smith A W, MacDougal and Rohatgi A 1991 *J. Appl. Phys.* 70 881

[8] Morris R G and Das S K 1992 *Int. J. Solar Energy* 12 95

[9] Brinkman A W, Al Allak H M, Arwan G R, Brown P D, Durose K, Ercelebi C, Simmons M V and Woods J 1992 *Int. J. Solar Energy* 12 233

[10] Das S K 1993 *Solar Energy Mater. Solar Cells* 29 227

[11] Tomita Y, Kawai T and Hatanaka Y 1993 *Japan. J. Appl. Phys.* 32 1923

[12] Bayhan H and Ercelebi C 1997 *Semicond. Sci. Technol.* 12 600

[13] Sakhaf M and Schmeits M 1996 *J. Appl. Phys.* 80 6893

[14] Schmeits M 1997 *Solid State Commun.* 12 1217

[15] Sze S M 1981 *Physics of Semiconductor Devices* (New York: Wiley)

[16] Chen J F, Chen N C, Wang P Y and Tsai M H 1996 *J. Appl. Phys.* 81 1255